Carbohydrate Polymers 100 (2014) 166–178

Contents lists available at ScienceDirect

Carbohydrate Polymers

journal homepage: www.elsevier.com/locate/carbpol

Antimicrobial wound dressing nanofiber mats from multicomponent (chitosan/silver-NPs/polyvinyl alcohol) systems

Abdelrahman M. Abdelgawad [a,*], Samuel M. Hudson [a], Orlando J. Rojas [b]

[a] Fiber and Polymer Science Program, College of Textiles, North Carolina State University, Campus Box 8301, NC, USA
[b] Department of Forest Biomaterials and Chemical and Biomolecular Engineering, North Carolina State University, Campus Box 8005, NC, USA

ARTICLE INFO

Article history:
Received 1 August 2012
Received in revised form 6 November 2012
Accepted 13 December 2012
Available online 29 December 2012

Keywords:
Silver nanoparticles
Chitosan
Electrospinning
Antimicrobial
Polyvinyl alcohol

ABSTRACT

Novel hybrid nanomaterials have been developed for antimicrobial applications. Here we introduce a green route to produce antibacterial nanofiber mats loaded with silver nanoparticles (Ag-NPs, 25 nm diameter) enveloped in chitosan after reduction with glucose. The nanofiber mats were obtained from colloidal dispersions of chitosan-based Ag-NPs blended with polyvinyl alcohol. Nanofibers (150 nm average diameter and narrow size distribution) were obtained by electrospinning and cross-linked with glutaraldhyde. The effect of crosslinking on the release of silver was studied by atomic absorption spectroscopy. Antimicrobial activity was studied by the viable cell-counting; mats loaded with silver and control samples (chitosan/PVA) with different degrees of cross-linking were compared for their effectiveness in reducing or halting the growth of aerobic bacteria. The results showed superior properties and synergistic antibacterial effects by combining chitosan with Ag-NPs.

1. Introduction

Nanomaterials and nanostructures may provide solutions to technological and environmental problems in the fields of water treatment, energy conversion, catalysis, and medicine (Dahl, 2007; Hutchison, 2008). The increased demand of nanoscale products must be accompanied by green synthesis methods. Green chemistry and green chemical processes are being integrated with recent developments in science and industry in attempts to reduce the generation of hazardous waste (Anstas, 1998). Related principles aim at minimizing the use of unsafe products and maximizing process efficiency while using environmentally safe solvents and nontoxic chemicals.

Compared to macroscopic or bulk materials the size, surface area and morphology of nanoparticles (NPs) endow them with unique physical and chemical properties (Kamyar, 2010). New applications of NPs and nanomaterials are emerging rapidly; for example, silver NPs have attracted extensive research as antimicrobial, antibacterial medical textiles and wound dressing materials (Choi, 2008; Hebeish, 2011; Rujitanaroj, 2008; Sharma, 2009). It is generally documented that Ag-NPs may attach to the cell wall, thus disturbing its permeability and inter-membrane exchange. The NPs may also penetrate inside the cell causing damage by interacting with phosphorus- and sulfur-containing biomolecules including DNA and proteins. Another possible mechanism is the release of silver ions from the NPs (Sambhy, 2006). Generally, silver does not adversely affect viable mammalian cells and cannot be easily resisted by microbes. Hence, silver has been incorporated into different materials in various forms and used in burn dressings to protect against microbial contamination (Brett, 2006).

Most of the synthetic methods of Ag-NPs reported to date rely on the use of organic solvents and toxic reducing agents that are highly reactive and pose potential environmental and biological risks, including hydrazine (Sakai, 2009), N,N-dimethylformamide (Pastoriza-Santos, 2002) and sodium borohydride (Van Hyning, 2001). Furthermore, the use of organic polymers as templates is considered as one of the most powerful and effective alternatives to synthesize Ag-NPs (Bŏzani', 2011; Konwarh, 2011). In addition to producing stable and well dispersed NPs with controlled size, shape and distribution, organic polymer also combine their intrinsic properties with those of the metal NPs. Earlier reports have dealt with biopolymers like chitosan (Huang, 2004), heparin (Yanli, 2008) and soluble starch (Vigneshwaran, 2006) as reducing and stabilizing agents for preparation of Ag-NPs.

Chitosan, a polysaccharide derived from naturally occurring chitin, displays unique polycationic, chelating, and film-forming properties due to the presence of active amino and hydroxyl groups. Chitosan is a well-known biopolymer that possesses antibacterial activity against Gram-negative and Gram positive bacteria, which has been exploited in a number of studies (Rabea, 2003). However, its mechanism of action against bacteria is still only partially

* Corresponding author at: 3114 College of Textiles, North Carolina State University, Campus Box 8301, NC, USA. Tel.: +1 919 8028027.
E-mail address: aabdelg@ncsu.edu (A.M. Abdelgawad).

0144-8617/$ – see front matter © 2013 Elsevier Ltd. All rights reserved.
http://dx.doi.org/10.1016/j.carbpol.2012.12.043

understood. Some hypotheses indicate that polycationic chitosan could interact with anionic groups on the cell surface thereby causing an increase in membrane permeability and probably disrupting and subsequently facilitating leakage of cellular proteins. Another mechanism suggested involves the formation of chitosan chelates with trace elements or essential nutrients resulting in the inhibition of the activity of enzymes (Rabea, 2003; Lim and Hudson, 2004). To date, chitosan has been reported to aid in the synthesis of metal nanoparticles, mainly gold and silver NPs (Dongwei Weia, 2009). However, to our knowledge only few studies have considered the use of chitosan–metal nanocomposites as antibacterial wound dressing material (Hang, 2010; Zhuanga, 2010).

Electrospun fiber mats have been reported to have great potential as wound dressings (Pillai, 2009; Zhou, 2006). Electrospinning is a process used to fabricate fibers using an electrically charged jet of diverse materials, including polymers with diameters ranging from several micrometers to several hundreds of nanometers. Because electrospun (e-spun) nanofibers have high porosity and a very small pore size, they have a larger specific surface area than that of cast films (Jia, 2007). Few reports have considered the combination of different mechanisms of antimicrobial action by designing hybrid materials. In particular, effective antimicrobial wound dressing nanocomposites based on chitosan nanofibers and Ag-NPs (Hang, 2010). Most of the preparation methods rely either on in situ reduction of Ag-NPs during the electrospinning process (Hang, 2010) or subsequent application of heat treatment to the nanomats (Rujitanaroj, 2008). In addition, these methods were suitable for low silver concentrations and not readily applicable for economical, larger scale production.

The aim of the present work is to combine Ag-NPs, embedded in chitosan, with polyvinyl alcohol (PVA) to produce antimicrobial nanofiber mats for wound dressing via a green method consisting of two steps: (1) preparation of Ag-NPs in high yields and highest possible concentration of enveloping chitosan with a green reducing agent and, (2) electrospinning of the chitosan-Ag-NPs/PVA blend. In order to improve the spinnability of the system the as-prepared colloidal solution of chitosan/Ag-NPs was blended with PVA in different blending ratios. Chemical cross-linking of the nanofibers was performed in order to maintain the integrity and morphology of the fibers and to control the release of the active ingredients from the mats. The fiber mats with the highest chitosan/Ag-NPs content were tested against *Escherichia coli*, which is considered one of the most widespread wound burn infectious bacteria.

2. Experimental

Chitosan, CS (M_v = 300 kDa and 85% degree of deacetylation) was obtained from Vanson^{TR} Company (USA). Polyvinyl alcohol, silver nitrate ($AgNO_3$), glucose, glacial acetic acid and glutaraldhyde solution (25%) were all laboratory grade reagents and purchased from Fisher Scientific (USA). Double distilled water was used in all experiments.

2.1. Chitosan-based Ag-NPs

Ag-NPs were prepared by means of simple chemical reduction of silver nitrate with glucose and chitosan as a reducing and protecting polymer. In a three-necked flask, 100 mL of chitosan solution (0.5–3%) dissolved in aqueous acetic acid (2%) was placed and a condenser was connected to one neck of the flask. The reaction was heated to the desired temperature (ranging from 25 °C to 95 °C) regulated with an oil bath. A given weight (0.045–0.72 g) of the metal precursor silver nitrate ($AgNO_3$) was dissolved in a minimum amount of distilled water (2 mL). The silver salt solution was added to the chitosan solution either one time, using a 10 mL plastic syringe, or drop-wise at a constant rate, using an automatic syringe. The solution was left for 5 min under continuous stirring (magnetic stirrer) to ensure uniform distribution of the metal precursor in the polymer solution. The concentration of the reducing agent, glucose, was calculated on the basis of molar ratio to the metal precursor concentration (1:0–1:10). The desired amount of glucose was dissolved in 3 mL distilled water and then dispensed to the reaction medium drop wise at a constant rate of 1.5 mL/h over 2 h time with via automatic syringe pump. The reaction was kept under stirring during given times (3–12 h). Following, the reaction vessel was left to cool down to room temperature. Chitosan Ag-NPs were placed in the refrigerator to stop any further silver reduction. Three different procedures were used: (1) single addition of metal precursor ($AgNO_3$) to the chitosan solution using a 10 mL syringe and addition over the course of 2 h time of the reducing agent (glucose) using the automatic syringe pump; (2) reverse sequence, i.e. metal precursor dispensed over 2 h time, and the reducing agent added to the chitosan solution at the beginning of the reaction and, (3) one time addition whereby all the materials were mixed at once and left to react till the end of the reaction time. Factors affecting the reduction efficiency and nanoparticle stability as well as shape and size are discussed in the text.

The ionic conductivity of PVA/CS-Ag-NPs and PVA/CS blend solutions was determined using a conductivity meter (Orion 162) under ambient atmosphere. The viscosity of each solution was measured using StressTech HR. viscometer at 25 °C.

2.2. Electrospinning of PVA/CS and PVA/CS/AgNPs

Ag-NPs prepared after the optimum chitosan-based preparation condition were used to electrospin nanofiber mats. Aqueous PVA solution (8 wt%) was mixed with chitosan-based Ag-NPs at various weight ratios (PVA/CS Ag-NPs): 100/0, 95/5, 90/10, 85/15, 80/20, 70/30, 60/40, and 50/50. PVA/CS samples were prepared at the same blending ratios for the purpose of assessment of the effect of Ag-NPs addition on spinnability and antimicrobial activity.

In a typical electrospinning process, each of the as-prepared solutions was loaded to 10-mL plastic syringe, the open end of which was attached to a blunt 22-gauge stainless steel hypodermic needle, which was used as nozzle. A GlassMan (WK series) high voltage source was used to charge the solution by attaching the emitted electrode of positive polarity to the nozzle, and the grounding one to the collector. The rate of spinning was 3 μL/min. The samples were collected on aluminum sheet wrapped around a rotatory collector of diameter (68 cm) for 48 h. An electrical potential of 25 kV was applied across a distance of 20 cm between the tip of the needle and the outer surface of the collector.

2.3. Cross-linking of fiber mats

Cross-linking of fiber mats of both PVA/CS and PVA/CS containing Ag-NPs was carried out using glutaraldehyde (GA). The fiber mats (10 cm × 30 cm) were attached to steel frames with paper binder clips and placed into a sealed chamber saturated with the vapor of 40 mL of GA solution. The nanofiber mats were exposed to GA vapor for given periods of time (30, 60, and 120 min) and then heat-treated in an oven at 70 °C under vacuum for 24 h to enhance the cross-linking reaction and to remove the unreacted GA.

2.4. Ag-NP detection and morphology analyses

UV–vis measurements were performed to confirm Ag-NPs formation. Varian UV–vis spectrophotometer operating in the absorbance mode was used. During the test the volume of the chitosan/silver-NPs was kept constant. FTIR was used to investigate the reduction effect of the chitosan. The chitosan-Ag-NPs colloidal

solution was freeze dried and then directly analyzed in a Nicolet FTIR spectrometer. All spectra were collected with a 2 cm^{-1} wavenumber resolution after 64 continuous scans. Atomic Absorption Spectroscope (AAS) was used to measure the actual quantity of silver present in the chitosan-Ag-NPs sample and to assess the release characteristics of as-loaded silver.

The morphology of the nanoparticles was examined using Transmission Electron Microscopy (TEM). A drop of aqueous chitosan/silver-NPs suspension was deposited on carbon-coated electron microscope grids and then allowed to dry in oven under vacuum for 24 h to ensure complete dryness of the sample. The grids were observed with a Hitachi HF2000 TEM operated at an accelerating voltage of 80 kV. The instrument was equipped with an energy-dispersive spectrum (EDS) to confirm the presence of silver metal. In addition, TEM was used to confirm the presence of the Ag-NPs in the electrospun nanofibers. Small amount of the nanofibers were collected on the copper grid during the electrospinning process. The morphology of the nanofibers in the electrospun mats was checked using field emission scanning electron microscopy (FE-SEM) using a JEOL 6400F microscope operated with an accelerating voltage of 5 kV and a working distance of 20 mm. A small portion of the nanofiber mat was fixed on conductive carbon tape and mounted on the support and then sputtered with an approximately 6 nm layer of gold/palladium (Au/Pd). The diameter and diameter distribution of the fibers in the mats were determined by using the Image J Tool for Windows version 3.0 with sample sizes of at least 50 fibers per SEM micrograph. Statistical analysis was performed using Microsoft Excel, one-way analysis of variance (ANOVA).

2.5. Loading and release capacity of fiber mats loaded with Ag-NPs

The amount of silver present in original suspension of chitosan/silver-NPs was quantified by taking 5 mL of the sample and dissolved in 10 mL of 50% nitric acid (HNO_3) then the volume was adjusted to 100 mL using double distilled water as a releasing medium. The concentration of silver was measured by Atomic Absorption Spectroscopy (AAS) and the results were reported as average values ($n = 3$). The release characteristics of silver from the PVA/CS-Ag-NPs fiber mats with 60/40 blend ratio were assessed. The specimens cut from the fiber mats samples (circular disc with 2.8 cm diameter) were immersed in 50 mL water at the skin physiological temperature of 32 °C at a given immersion periods between 0 and 7 days. The releasing medium was quantified for the amount of the released silver, using AAS. Each measurement was carried out in triplicate and the cumulative amount of released silver determined. The cumulative release profiles of silver were expressed as unit weight of the samples cross-linked during different GA treatment times (30, 60 and 120 min).

2.6. Antibacterial activity

The antibacterial activity of the fiber mats against *Escherichia coli* (*E. coli*) Gram negative bacteria, which is commonly found on burn wounds, was measured by using the viable cell counting method. Briefly, about 100 μL *E. coli* was cultivated in 100 mL of a nutrient broth solution, to give a bacterial concentration of about 7×10^{11} CFU/mL. After this, 1 mL of the bacteria/nutrient solution was added to 9 mL of sterilized nutrient broth solution (0.8%). Several decimal dilutions were performed until the bacterial concentration increased from 7×10^3 to 7×10^7 CFU/mL. Two different bacteria concentrations were selected for use, 7×10^5 and 7×10^7 CFU/mL. PVA/CS and PVA/CS/Ag-NPs systems with blend ratios of 90/10, 80/20, and 60/40 were used in the antibacterial tests. The weight and size of the fiber mats of PVA/CS or PVA/CS/Ag-NPs were 100 mg as disks of 2.8 cm diameter. To perform the antibacterial testing, the respective fiber mats were put into 10 mL of the bacteria/nutrient solution incubated in a shaker at 37 °C for 12 h. After the exposure of the bacteria to fiber mats, 100 μL of the bacterial solution was taken out and quickly spread on a plate containing nutrient agar. Plates containing bacteria were incubated at 37 °C for 24 h, and then the numbers of the surviving colonies were counted. These results were compared to the number of bacteria colonies of the untreated control that had not been exposed to the fiber mats.

3. Results and discussion

3.1. Preparation of chitosan-based Ag-NPs

It is expected that the effect of natural polymers in the preparation of colloidal Ag-NPs is governed by a number of factors such as water solubility, degree of polymerization and reduction power. The reaction mechanism for the synthesis of Ag-NPs and their stabilization has been discussed previously (Goia, 2004; Hebeish, 2010). For example, linear and dendritic polymers have been successfully used for NP synthesis. Polyhydroxylated macromolecules present interesting dynamic supramolecular associations facilitated by inter and intra-molecular hydrogen bonding resulting in capsules, which can act as templates for nanoparticles growth. With this in mind, medium molecular weight chitosan was chosen in the present study.

We noted that the reaction temperature, reduction time, silver salt and chitosan concentration, glucose/$AgNO_3$ molar ratio, and sequence of addition were some of the factors affecting the reduction efficiency and stability as well as the shape and size of Ag-NPs. Such factors along with the involved mechanisms were investigated in order to optimize the chitosan/glucose/$AgNO_3$ system formulation and to achieve a green route for the fabrication of antibacterial fiber mats.

3.1.1. Formation of Ag-NPs and interactions with chitosan

When $AgNO_3$ is mixed with chitosan solution, Ag^+ ions could bind to chitosan probably via electrostatic (i.e. ion-dipole) interactions, because the electron-rich oxygen atoms of the hydroxyl and glucosidic groups of chitosan are expected to interact with electropositive transition metal cations. Such interactions cause a change of the color of the chitosan colloidal solution upon the addition of $AgNO_3$, from a clear pale yellow to a milky white. Subsequently silver ions oxidize the hydroxyl groups of chitosan to carbonyl groups and as a result the silver ions are reduced to elemental silver. In addition, the added glucose supports the reduction power of chitosan by offering more active sites for oxidation through its free aldehydic groups. Similar observations were reported previously for starch (Vigneshwaran, 2006), hydroxypropyl cellulose (Abdel-Halim, 2011), and carboxymethyl cellulose (Hebeish, 2010).

The specific interaction of chitosan with the surface of the metal was followed by FTIR measurements on films of pure chitosan and chitosan–Ag-NPs. The figure (displayed in the Supplementary Material file) shows two representative FTIR spectra which contain the main vibrational bands of chitosan. Although there is a possibility of overlapping between the N—H and O—H stretching vibrations, the strong broad band at 3300–3500 cm^{-1} is characteristic of the N—H stretching vibration. The significant change in the shape of this band (3359.8 cm^{-1}) indicates that the N—H vibration was affected by the attachment of silver. The band at 1559.4 cm^{-1} assigned to the amino group in pure chitosan film shifted to a lower wavenumber 1510 cm^{-1} in the presence of Ag-NPs. In addition, the characteristic bands at 1652.9 cm^{-1} (amide I band characteristic to

C=O stretching of N-acetyl group) was shifted to lower wavenumber 1636.9 cm^{-1}. However, bands at 1409 cm^{-1} (bending vibration of OH group), 1376 cm^{-1} (symmetric deformation vibration mode of CH_3), and 1323 cm^{-1} (CH_2 wagging vibration mode in primary alcohol) were not affected by the presence of the metal. This clearly identifies the involvement of primary amino and amide groups in the interaction with the metal; it is expected that the amino groups acted as capping sites for the Ag-NPs. Similar results were reported previously by others (Dongwei Weia, 2009; Potara, 2011).

3.1.2. Effect of reaction temperature and time

Various temperatures were used during the preparation of Ag-NPs, and typical UV–vis absorption spectra of the resulting solutions are shown in Fig. 1a. The data indicate that up to 70 °C the Ag^+ reduction efficiency was not significant and formation of Ag-NPs was very limited. Increasing the reaction temperature above, to 80–95 °C leads to significant enhancement in the characteristic surface plasmon resonance (SPR) band of Ag-NPs centered at about 420 nm, indicating the formation of Ag-NPs.

Fig. 1b shows the UV–vis absorption spectra of Ag-NPs colloidal solutions prepared after different reaction times. It can be observed that (i) at the early stages of the reaction (after 3 h) the plasmon band is broaden and simple test for silver ion using NaCl solution indicates low conversion of silver ions to metallic Ag-NPs; (ii) extending the reaction time to up to 7 h leads to significant enhancement of the plasmon intensity, indicating that large amounts of silver ions are reduced and formed clusters; (iii) further increase in the reaction time, up to 10 h, was accompanied by insignificant increase in the absorption intensity. Fig. 1c shows the TEM micrographs and the particle size distribution histograms of Ag-NPs formed after 3 h and 7 h. The corresponding size distribution histograms indicated that the size of the Ag particles is in the 10–15 nm and 25–30 nm ranges, respectively. This in turn suggests that the formation of silver seeds during the first 3 h of the reaction and then the growth step starts.

3.1.3. Effect of silver nitrate/reducing agent molar ratio, glucose and chitosan concentrations

Fig. 2a shows the UV–vis spectra of Ag-NPs colloidal solutions prepared using different Ag^+/glucose molar ratios (1:0–1:16 Ag^+/glucose). The data indicate that the intensity of the maximum absorbance peak at 420 nm increases as the Ag^+/glucose ratio increases up to 1:4; further increases in the glucose concentration did not produce any significant upturn in the peak intensity. Fig. 2b shows the TEM micrograph and the Ag-NPs formed (1:4 molar ratio condition). The corresponding size distribution histogram indicated that the size of the formed NPs is in the 25–30 nm range.

Fig. 2c shows the UV–vis absorption spectra of Ag-NPs prepared using chitosan at different concentrations (0–3%, w/v, initial pH of 2.5, 95 °C, 7 h reaction time). The intensity of the surface plasmon resonance peak increases with the solution concentration of chitosan. In the absence of chitosan, no significant absorbance was observed which indicates that there was no substantial reduction occurred. When the concentration increased up to 0.5% (w/v) a low intensity, bell shaped plasmon band at 424 nm appeared, which is taken as indication of the formation of Ag^0 nanoparticles. Further increase in chitosan concentration, above 0.5% (w/v) leads to characteristic increases in the peak absorbance intensity. Above such concentration, and regardless of the chitosan concentration used, similar plasmon bands are observed at 420 nm wavelength. It is worthy to mention that the increase in the absorption intensity, by increasing the chitosan concentration up to 3% could be ascribed to increasing the reducing power and the enhancement in the stabilization efficiency of the formed Ag-NPs.

It is also worthy to mention her, that when 3% (w/v) chitosan was applied, there is a limitation to increase the glucose concentration above 1:2 molar ratios. Any increment above that concentration would result in gel formation. This may be attributed to the network crosslinking between glucose and chitosan and Ag^+ under high temperature and agitation. Fig. 2d shows the TEM image and the particle size distribution histograms of Ag-NPs formed using 1.5% and 3% chitosan (w/v). The corresponding size distribution histogram (not shown) indicated that the size of the formed Ag-NPs was in the range of 25–30 nm for both concentrations.

Silver ion complexation and reduction by polysaccharides is complex and involves more than one mechanism. For the synthesis of Ag-NPs, the generally accepted mechanism suggests a two-step process, i.e. atom formation and then polymerization of the atoms. In the first step, a portion of metal ions in a solution is reduced by the available reducing groups of chitosan and glucose. Herein, glucose was used to support the reduction power of chitosan. The atoms thus act as nucleation centers and catalyze the reduction of the remaining metal ions present in the bulk solution. Subsequently, the atoms coalesce leading to the formation of metal clusters. The surface ions are again reduced and in this way the aggregation process does not cease until high values of nuclearity are attained, which results in larger particles. The process is stabilized by the interaction with the polymer so preventing further coalescence (Goia, 2004).

3.1.4. Effect of order of addition

The metal precursor (silver nitrate) dissolved in 2 mL deionized water then added to the reaction medium using automatic pump over 1 h. In such case more silver NPs were produced in the nucleation step (first 3 h) due to the high concentration of the reducing agent, glucose, in the medium. So that it shows absorbance peak intensity larger than that produced from regular addition technique after 3 h. On the other hand, in the one-time addition technique, in which all the reagents mixed together at the beginning of the reaction, more silver NPs produced in the nucleation step (first 3 h) due to the presence of glucose and silver ions in high concentration (the whole amounts). More nuclei were formed in the nucleation step during the first 3 h and then growth takes place overtime. It was found that (figure shown in the Supplementary Material file) one time addition procedure produced the highest concentration of silver NPs after 7 h of reaction. A surface plasmon peak was observed at 422 nm with highest absorbance intensity.

3.1.5. Effect of silver nitrate concentration

Several studies have been conducted on scaling up the process of fabrication of Ag-NPs (Hebeish, 2010). Results of the foregoing section made it possible to prepare Ag-NPs with concentration of *ca.* 4500 ppm. Interests in preparation of Ag-NPs solutions, which acquire higher concentrations of the nanosized silver particles are, therefore, stimulated. Thus a study was undertaken where silver nitrate ($AgNO_3$) was incorporated at different concentrations in the reaction medium. The UV–vis spectra of Ag-NPs resulting from incorporating different amounts of $AgNO_3$ (0.045–0.72 gm/100 mL chitosan solution) and keeping chitosan concentration constant at 1.5% for all $AgNO_3$ concentrations reveals that similar absorption spectra were obtained at wavelength 420 nm and that the intensity of the absorption peak increased by increasing $AgNO_3$ concentration in the reaction medium. It is concluded, that in order to obtain Ag-NPs colloidal solutions with concentrations higher than 4000 ppm (*ca.*), one should use an $AgNO_3$:chitosan ratio of 0.72 g: 1.5 g per 100 mL solution. The UV–vis spectrum is shown in the Supplementary Data file.

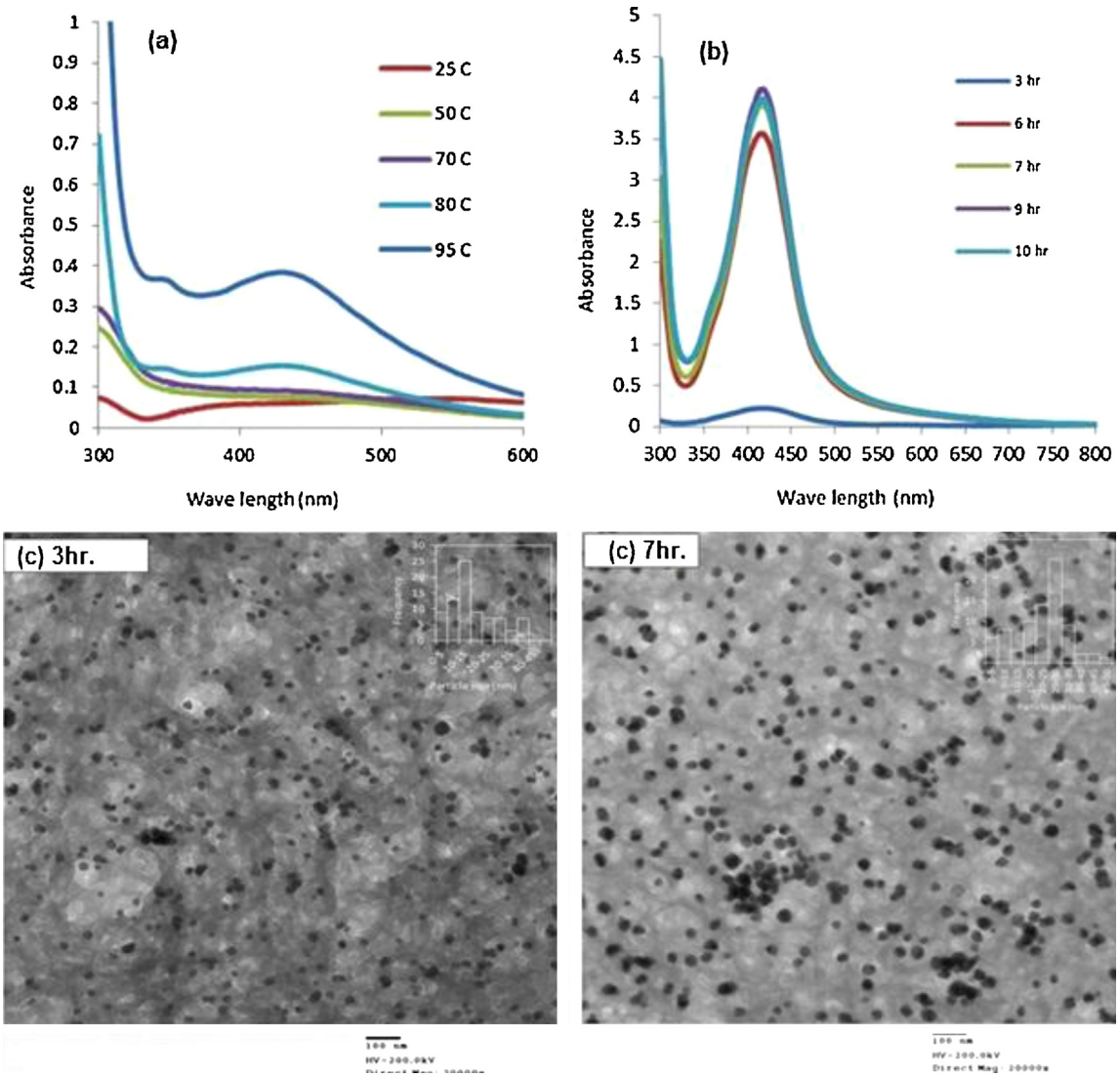

Fig. 1. (a) UV–vis spectra of Ag-NPs prepared at different temperatures. Reaction conditions: chitosan conc. (1.5%); $AgNO_3$ conc. (0.045 g/100 mL); Ag^+/glucose molar ratio (1:10); reaction duration (7 h); mode of addition (regular addition)]. (b) UV–vis spectra of Ag-NPs prepared at different reaction durations. Reaction conditions: temperature (95 °C); chitosan conc. (1.5%); $AgNO_3$ conc. (0.36 g/100 mL); Ag^+/glucose molar ratio (1:4); mode of addition (regular addition)], (c) TEM micrographs and the particle size distribution histograms of Ag-NPs formed after 3 h and 7 h.

3.1.6. The optimum conditions for nanoparticles preparation

The optimum conditions were selected to prepare highly concentrated Ag-NPs colloidal solutions, based on the natural capping agent chitosan: 95 °C, 2% (w/v) chitosan concentration; 0.72 gm (*ca.* 4500 ppm) $AgNO_3$ concentration, 7 h reaction time; 1:4 Ag^+/glucose molar ratio and regular addition procedure. Fig. 3a represents the UV–vis spectra of Ag-NPs under these conditions. A high intensity absorbance band is observed at 427 nm (Abs. 4) indicating the formation of Ag-NPs in large concentrations. The exact concentration of the produced Ag-NPs has been estimated using the Atomic Absorbance Spectroscopy (AAS) technique and discussed later. Fig. 3b shows the TEM micrograph and the particle size distribution histograms of Ag-NPs formed using the optimum conditions. The corresponding size distribution histogram clearly illustrates that the size of the formed particles seem to be identical and in the range of 20 ± 5 nm. Fig. 3c shows the EDS chart which confirms the presence of silver metal.

Several issues can be highlighted: (1) reaction temperature is very critical for the reduction process and 95 °C is the optimum temperature for preparation of Ag-NPs; (2) as the concentration of the metal precursor increases the formation of nanoparticles increase until it reaches the agglomeration concentration; (3) chitosan has reducing power and its presence as capping agent helps to form and protect from coalescence Ag-NPs; (4) the presence of the reducing agent (glucose) is critical to increase the efficiency of the reduction power of chitosan; (5) the reducing agent may help to initiate the reduction so that the nucleation process starts earlier; (6) the new formed silver nano-clusters might act as a catalyst for the reduction of the remaining silver ions; (7) as the concentration of the capping agent, chitosan, increases the reduction power upturns and the particle size distribution decreases due to particle stabilization; (8) one time addition of the reducing agent helps the nucleation step to take place faster; (9) the ratio between chitosan: silver nitrate: glucose should remain in certain range in order to avoid gel formation.

3.2. Electrospun fiber mats of PVA/CS and PVA/CS/Ag-NPs

The best preparation conditions of chitosan-based Ag-NPs were applied to produce nanofiber mats via electrospinning. Chitosan itself is difficulty fabricated by the electrospinning process using the regular solvents because of its polycationic nature in solution.

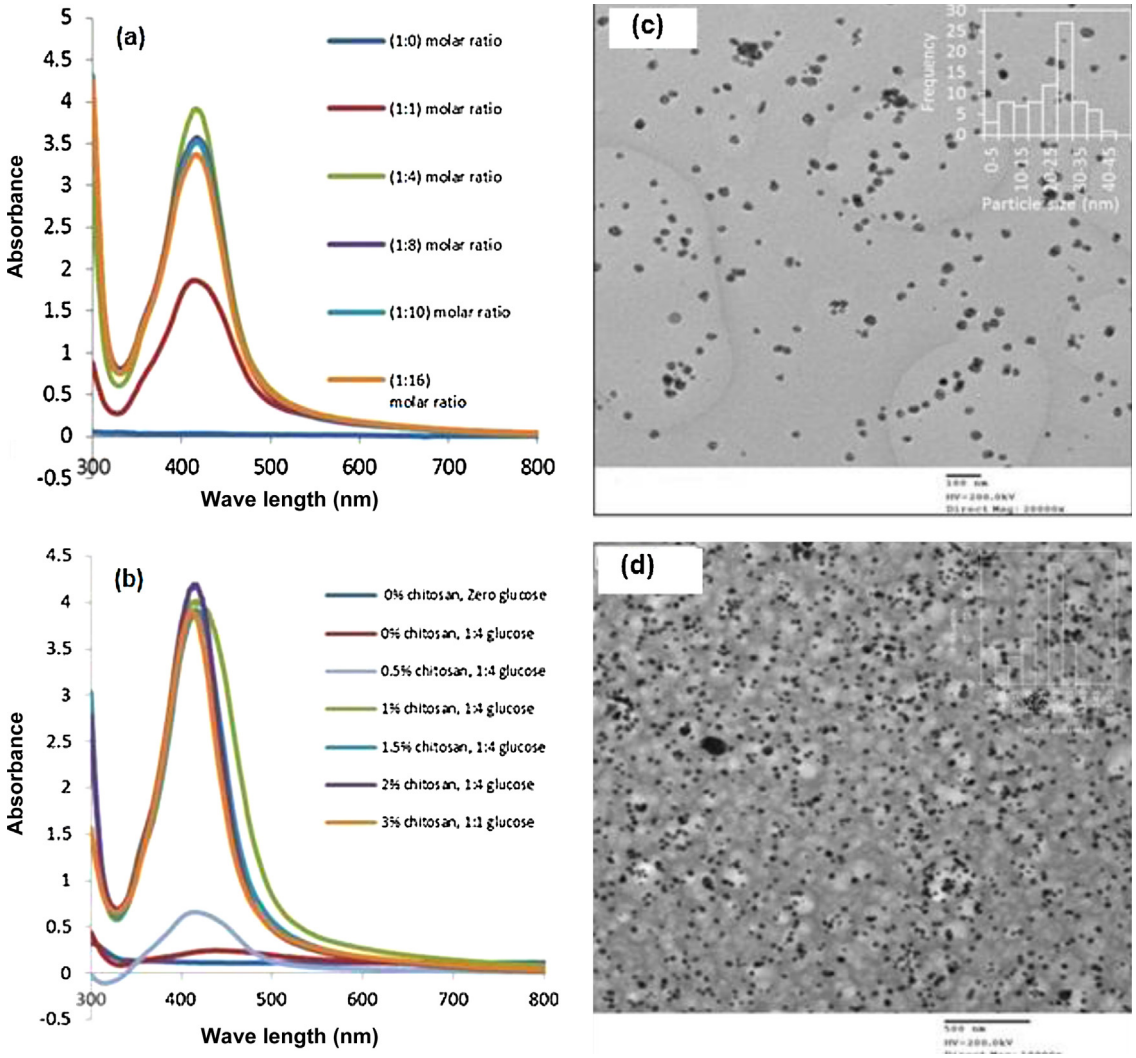

Fig. 2. (a) UV–vis spectra of Ag-NPs prepared at different Ag^+/glucose. Reaction conditions: temperature (95 °C); chitosan conc. (1.5%); $AgNO_3$ conc. (0.36 g/100 mL); reaction duration (7 h); mode of addition (regular addition)]. (b) TEM micrograph and the particle size distribution histograms of Ag-NPs formed under 1:4 molar ratio conditions. (c) UV–vis spectra of Ag-NPs prepared at different chitosan concentrations. Reaction conditions: temperature (95 °C); reaction duration (7 h); $AgNO_3$ conc. (0.36 g/100 mL); Ag^+/glucose molar ratio (1:4); mode of addition (regular addition)], (d) TEM micrograph and the particle size distribution histograms of Ag-NPs formed using 1.5% chitosan.

To overcome this short coming of chitosan, many researchers have sought to improve its electrospinning ability by mixing chitosan with other polymers such as poly(vinyl pyrrolidone) (PVP) (Ignatova, 2006), poly(ethylene oxide) (PEO) (An, 2009), and poly(vinyl alcohol) (PVA) (Hang, 2010). This latter polymer has been also extensively used by us to produce electrospun fiber mats with high mechanical integrity (Peresin, 2010). Therefore, PVA was dissolved in distilled water at concentration of 8 wt% then mixed with chitosan-based Ag-NPs at various weight ratios (PVA/CS-Ag-NPs): 100/0, 95/5, 90/10, 85/15, 80/20, 70/30, 60/40, and 50/50. PVA/CS samples were prepared at the same blending ratios for the purpose of assessment of the effect of Ag-NPs addition on the fiber spinnability and antimicrobial activity.

The performance and morphology of the e-spun fiber mats were affected by many factors, including the physicochemical properties of the polymer solution and the electrospinning process parameters. The viscosity and ionic conductivity of polymer solutions are considered to be major parameters in electrospinning (Zhou, 2006; Peresin, 2010). In this study, measurements were performed on the viscosity and ionic conductivity of the PVA/CS as well as PVA/CS-Ag-NPs blends at various concentrations of CS in the polymer solutions (Fig. 4). It is found that the ionic conductivity of the polymer solutions increased with the CS content due to its – NH_3^+ groups that evolve from – NH_2 in the acetic acid solution. In addition, the same trend was observed for the PVA/CS-Ag-NPs solutions, as shown in Fig. 4a, but with higher conductivity values which may be attributed to the presence of silver-NPs and silver ions.

Fig. 4b illustrates the effect of the chitosan (CS) and the presence of Ag-NPs in the solution viscosity in PVA/CS and PVA/CS-Ag-NPs systems. The increase in the viscosity of a polymer solution with an increase in the CS content is due to the high viscosity of the CS and to the effect of the intermolecular interactions between the PVA and CS, such as hydrogen bonding in the solution state (Jia, 2007). However, the viscosity is decreased in the case of PVA/CS-Ag-NPs blends, which may be attributed to the preparation procedure: During the reduction of Ag^+ ions in the preparation step chitosan may undergo degradation to certain extent due to the redox reaction and the heat treatment.

Fig. 5 shows FE-SEM micrographs, average diameter, and diameter distribution of the fiber mats made of the PVA/CS blend e-spun fibers at different weight ratios of PVA to CS. As shown in Figs. 5(a)–(f), a defect-free fibers are observed in mats with PVA to CS weight ratio of up to 70/30. The e-spun fibers in the fiber mats beaded and became irregular in shape at PVA to CS weight

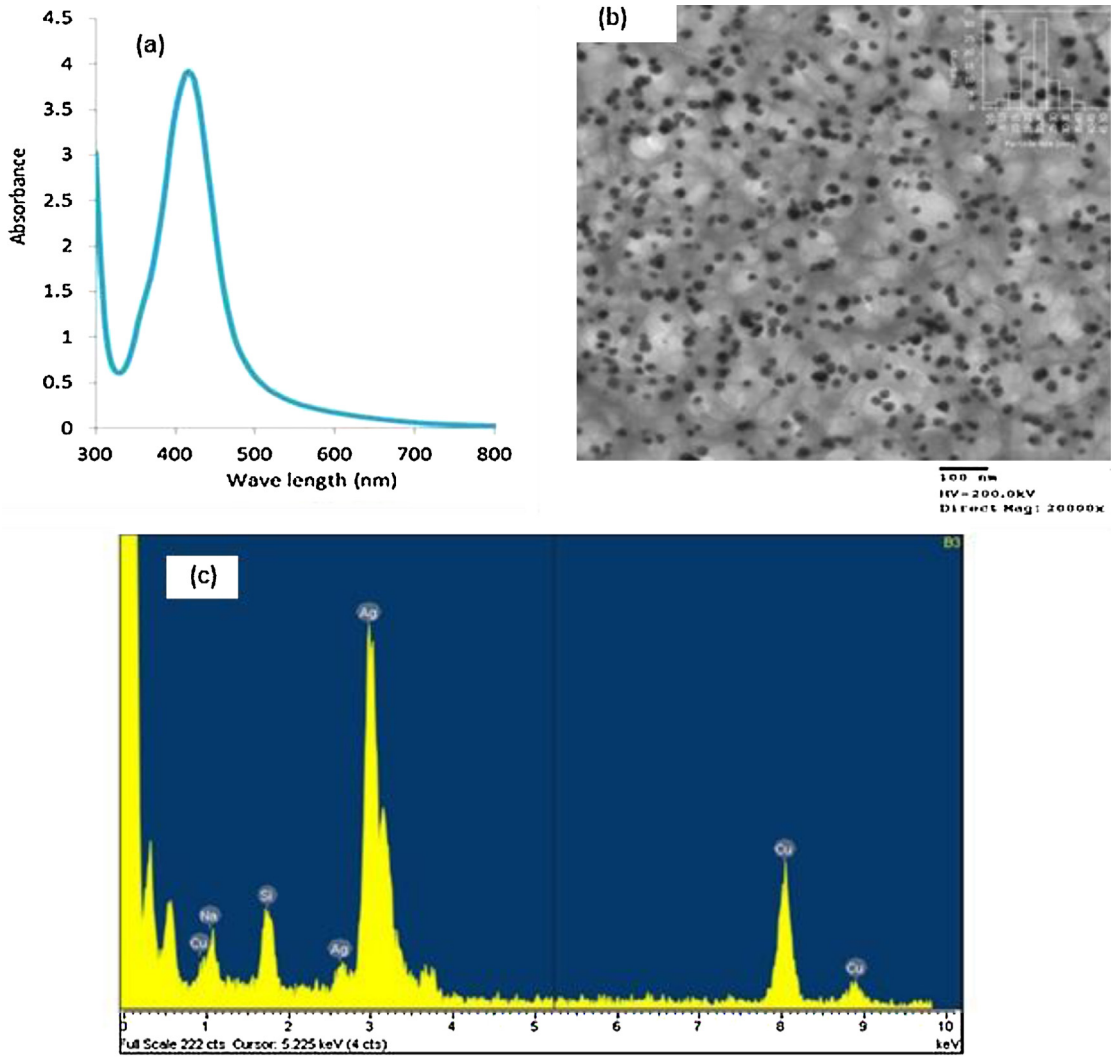

Fig. 3. (a) UV–vis spectra of Ag-NPs prepared under the optimum conditions. Reaction conditions: temperature (95 °C); reaction duration (7 h); $AgNO_3$ conc. (0.72 g/100 mL); chitosan concentration (2%, w/v); Ag^+/glucose molar ratio (1:4); mode of addition (regular addition)], (b) TEM micrograph and the particle size distribution histograms of Ag-NPs. (c) EDS chart of the formed silver-NPs.

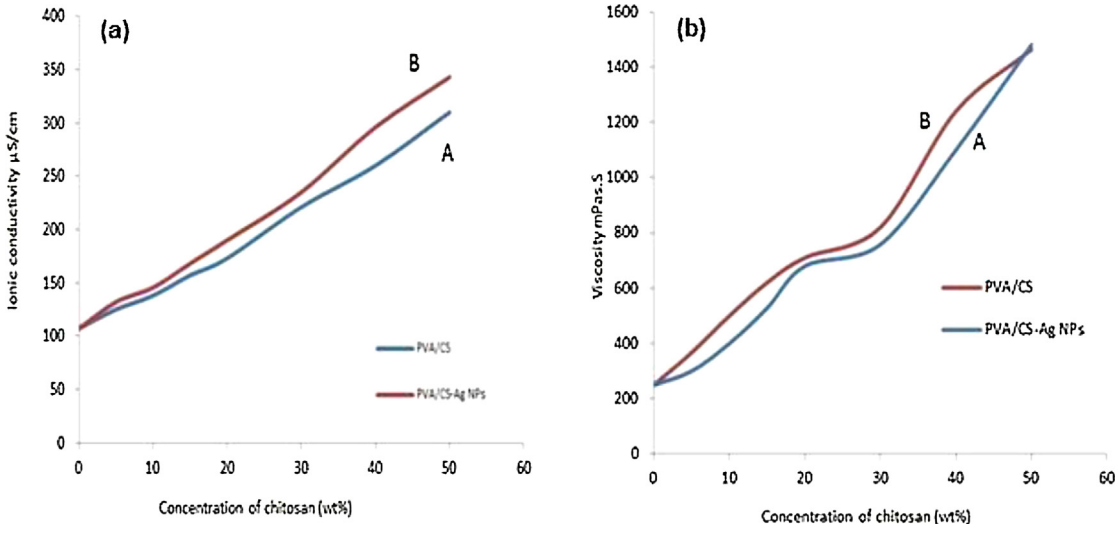

Fig. 4. (a) Ionic conductivity of the PVA/CS and PVA/CS-Ag-NPs blend solutions. (b) The effect of the CS content and the presence of Ag-NPs in the polymer solution on the viscosity of polymer solutions of the PVA/CS [A] and PVA/CS-Ag-NPs [B] blend solutions.

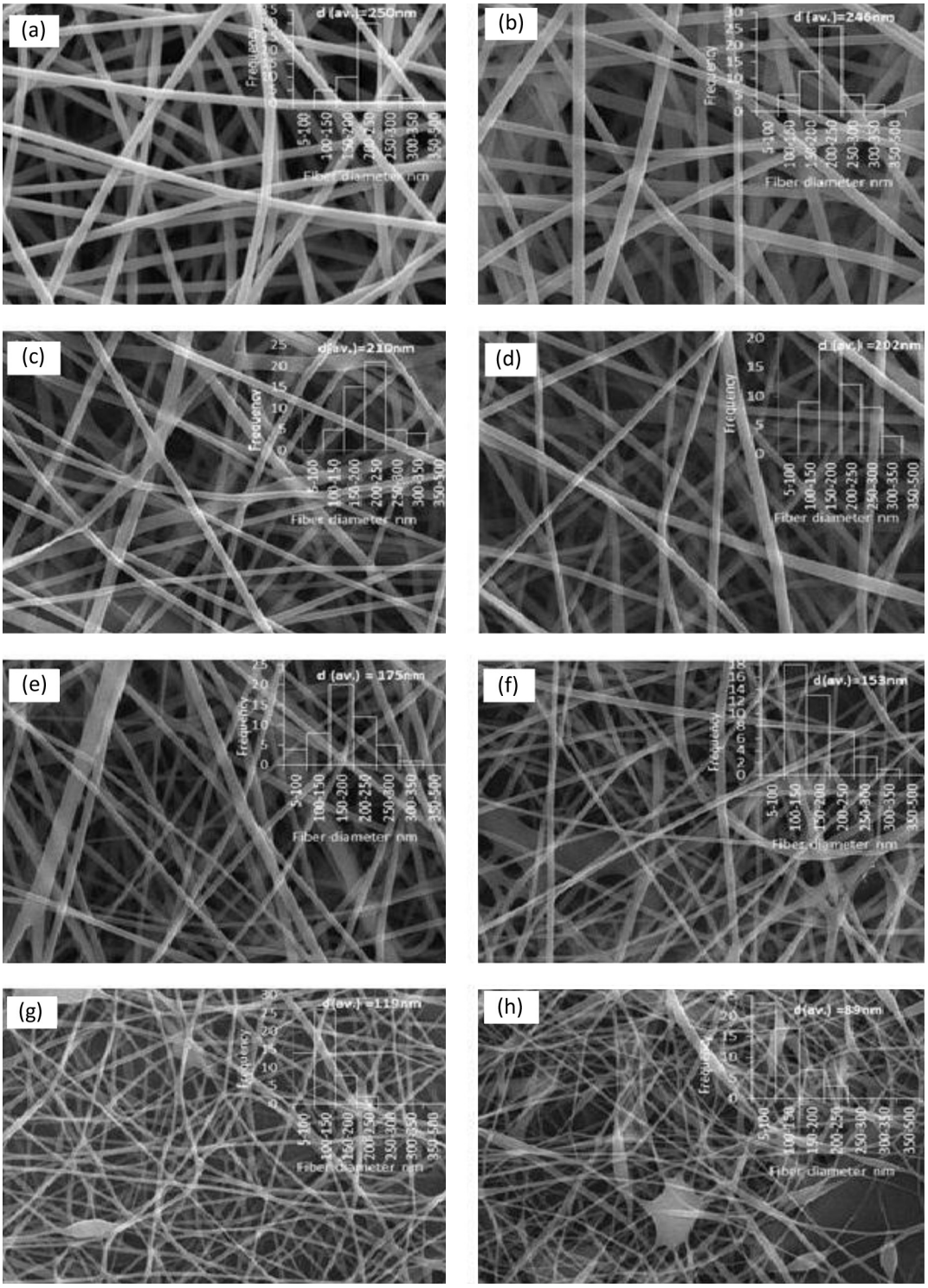

Fig. 5. FE-SEM micrographs, average diameter, and diameter distribution of the e-spun mats made of the PVA/CS blend e-spun fibers at different weight ratios: (a) Neat PVA; (b) 95/5; (c) 90/10; (d) 85/15; (e) 80/20; (f)70/30; (g) 60/40; and (h) 50/50.

ratios 60/40 and 50/50, as can be seen in Fig. 5(g)–(h). When the CS content in the PVA/CS blend was higher than 50 wt%, e-spun fibers could hardly be formed. These observations can be explained by the fact that when the concentration of the chitosan (a polycation) in the blend solution increases, the repulsive force between the cationic groups within the polymer's backbone increases. Thus, the formation of continuous fibers is inhibited during the electrospinning process under a high electric field. Simultaneously, as the concentration of CS in the blend increases from 0 to 50 wt%, the average diameters of PVA/CS blend e-spun fibers decreases from 250 nm to 89 nm, and the diameter distribution become slightly narrower. This is explained by the effect of CS which leads to the increased charge density on the surface of the ejected jet formed during electrospinning (Park, 2004).

Fig. 6 shows FE-SEM micrographs of the fiber mats of the PVA/CS-Ag-NPs blends with different PVA to CS weight ratios, their

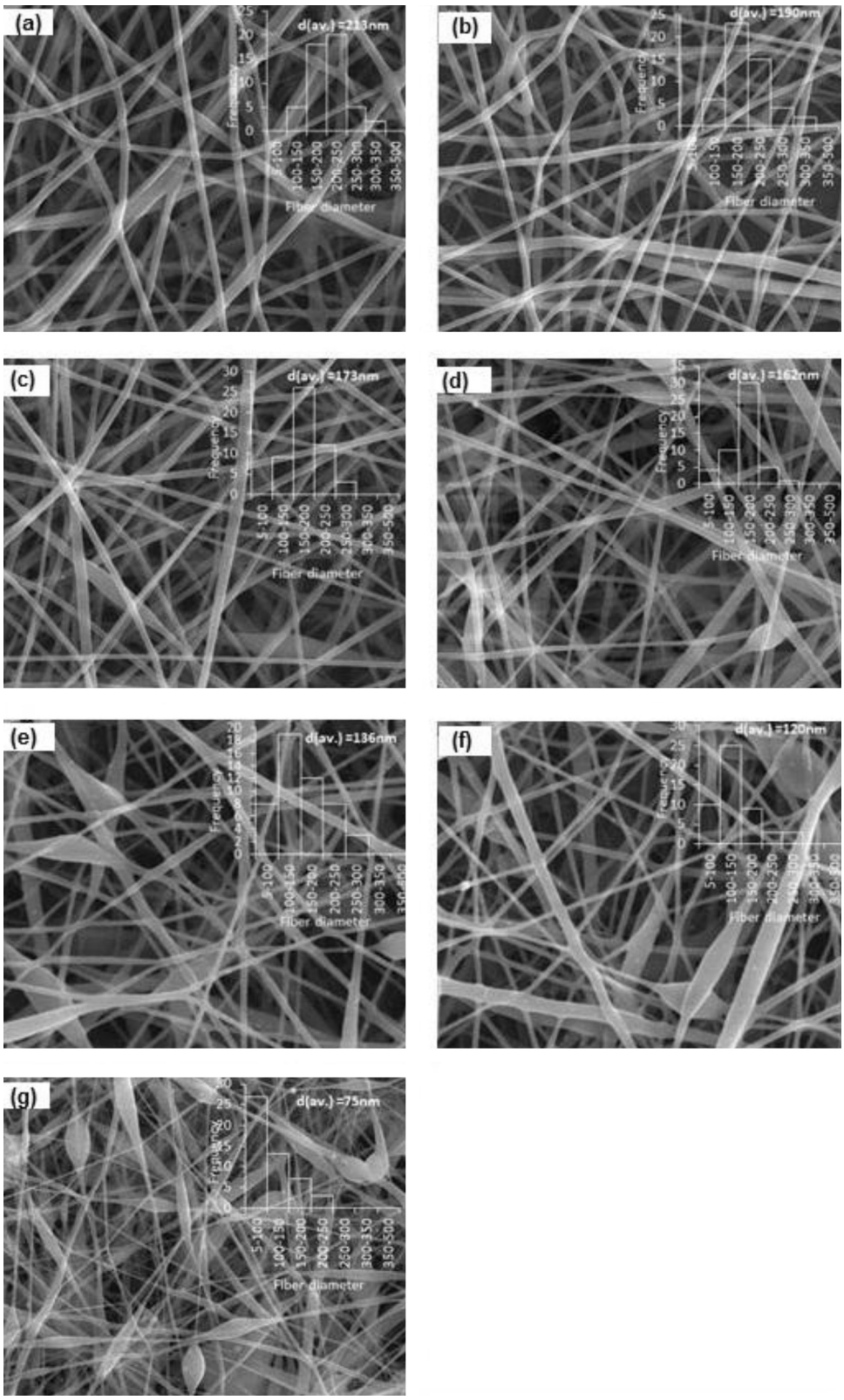

Fig. 6. FE-SEM micrographs, average diameter, and diameter distribution of the e-spun mats made of the PVA/CS-Ag-NPs blend e-spun fibers at different weight ratios: (a) 95/5; (b) 90/10; (c) 85/15; (d) 80/20; (e) 70/30; (f) 60/40; and (g) 50/50.

average diameter and diameter distribution. Both samples, with and without Ag-NPs, presented the same behavior but the average diameter of the e-spun fibers in a PVA fiber mat containing Ag-NPs was found to be smaller than those with PVA/CS. The fiber diameter was in the range of 213 nm to 75 nm.

Comparing Figs. 5 and 6, it can be observed that the diameters of the e-spun fibers of the fiber mats tend to decrease when the CS content in the polymer blend solutions increases. No beading was observed in the fiber mats of the PVA/CS-Ag-NPs blends at PVA to CS-Ag-NPs weight ratios of 95/5, 90/10, 85/15, and 80/20, as shown

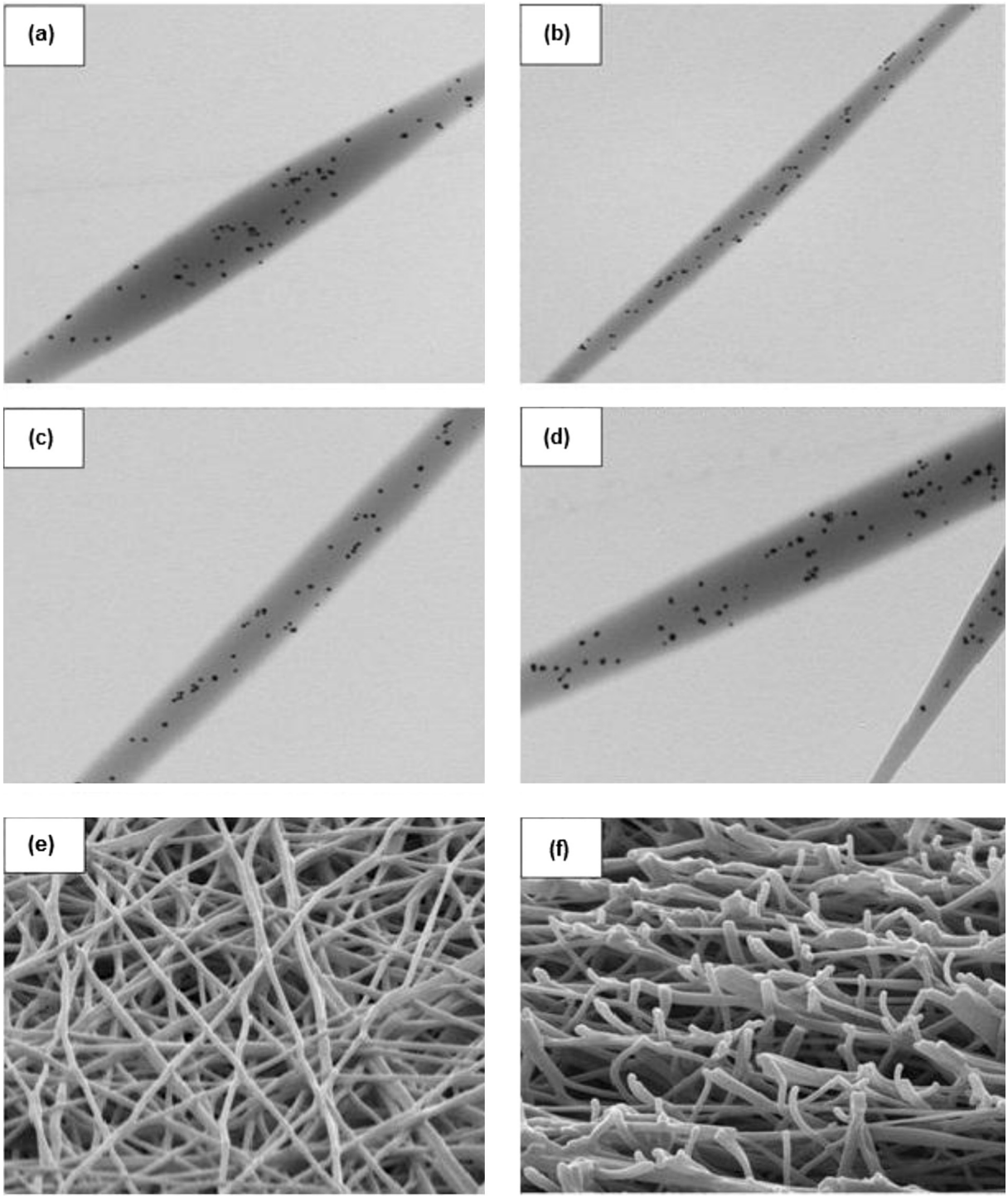

Fig. 7. TEM micrographs of e-spun fibers of 60/40 (weight ratio) PVA/CS-Ag-NPs, (a–d) micrographs show individual PVA/CS-Ag-NPs fibers loaded with Ag-NPs; (e) PVA/CS-Ag-NPs nanofiber mat top-view; and (f) cross-section of PVA/CS-Ag-NPs nanofiber mat.

in Fig. 6(a)–(d). Whereas, in the weight ratios of 70/30, 60/40, and 50/50 beading occurred and increased with the CS-Ag-NPs ratio. The microstructure of these fiber mats was different from that of the PVA/CS mats shown in Fig. 5. Since the viscosity of the PVA/CS-Ag-NPs blend solutions were lower than that of PVA/CS blend solutions, the beads started to appear in the 70/30, 60/40, and 50/50 blends. Hence, the presence of Ag-NPs in the PVA/CS solution improved the electrospinning ability of PVA/CS blend solutions in terms of fiber diameter. On the other hand, the fiber uniformity was affected by the method of preparation. However, fibers of 60/40 PVA/CS-Ag-NPs has some beaded structures but still have good uniformity and contains high Ag-NPs loading. The presence of Ag-NPs in the matrices clearly improved its morphology and fiber spinnability.

Fig. 7 shows the TEM micrographs of fibers of 60/40 PVA/CS-Ag-NPs weight ratio. Fig. 7(a)–(d) represents an individual fiber contains Ag-NPs on the surface of the fiber. The nanofibers in the mats kept its morphology after cross-linked with glutaraldhyde as clear from Fig. 7(e) and (f).

3.3. Silver loading and release from e-spun fiber mats

Fiber mats were cross-linked for 30, 60, and 120 min and the actual amount of silver that was present in the chitosan-Ag-NPs sample was determined. The theoretical content of Ag-NPs in the original sample was calculated to be 0.4560 g/100 mL chitosan solution (456,000 ppm). To determine the amount of silver that was actually present in the sample and hence, the reduction efficiency, 5 mL of the sample dissolved in 10 mL of 50% nitric acid (HNO_3) then digested in the microwave for 2 h followed by adjusting the volume to 100 mL using double distilled water as a releasing medium. The obtained silver-containing solution in such media was then determined for the actual content of silver-NPs (by means of AAS) to be 0.3142 g/100 mL (i.e. 3142 ppm). This accounted for very close to 70% of the initial, theoretical content of silver-NPs. The rest of the sample may be remained in the form of Ag^+ or have been oxidized to silver oxide.

The release characteristic of Ag^+ ions from the 30, 60, and 120 min cross-linked fiber mats was investigated by the total immersion method in distilled water for a period of up to 7 days. The cumulative amount of Ag^+ ions released from these materials is reported in Fig. 8. The results were measured in part per million units (ppm) then divided by the actual weight of

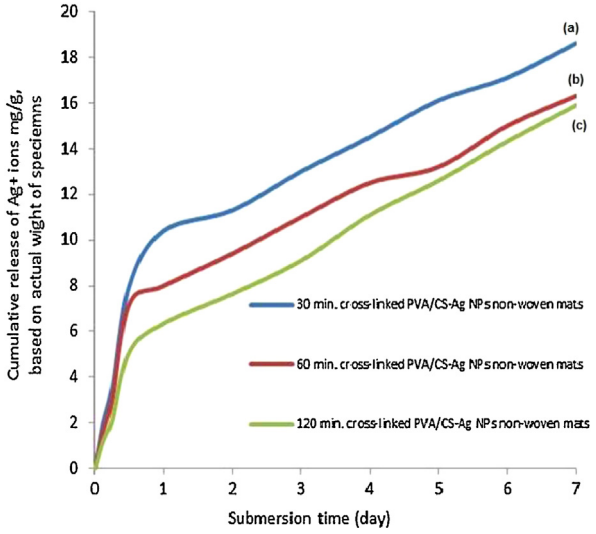

Fig. 8. Cumulative release profiles of Ag^+ ions from (a) 30 min. cross-linked fiber mats; (b) 60 min. cross-linked fiber mats; and (c) 120 min. cross-linked fiber mats in distilled water for a period of time ranging from 0 to 7 days at the skin physiological temperature of 32 °C.

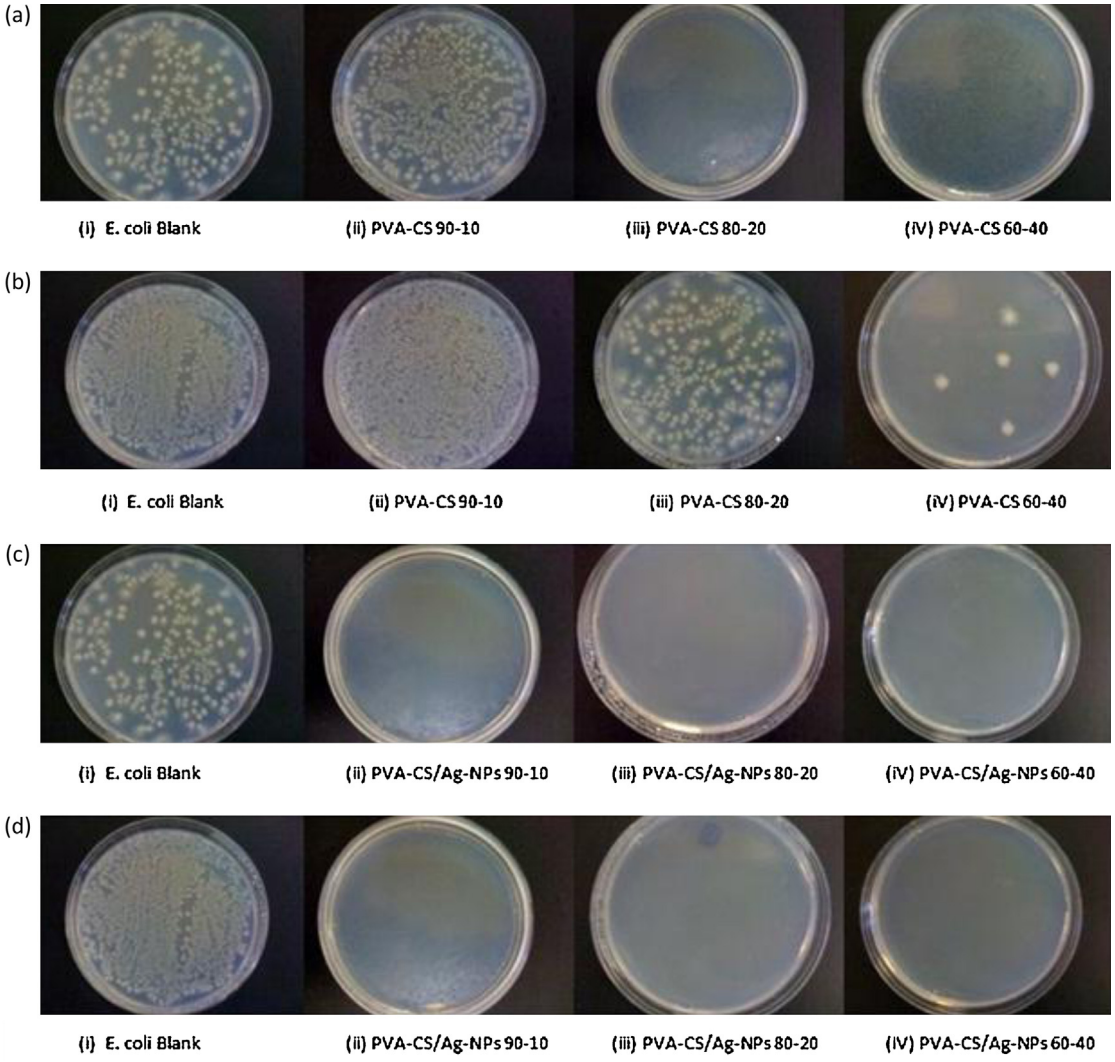

Fig. 9. The antibacterial activity of the e-spun mats against *E. coli*. (a) PVA/CS [9/10, 80/20, and 60/40] weight blending ratios at 7×10^5 CFU/mL bacteria, (b) PVA/CS [9/10, 80/20, and 60/40] weight blending ratios at 7×10^7 CFU/mL bacteria, (c) PVA/CS-Ag-NPs [9/10, 80/20, and 60/40] weight blending ratios at 7×10^5 CFU/mL bacteria, and (d) PVA/CS-Ag-NPs [9/10, 80/20, and 60/40] weight blending ratios at 7×10^7 CFU/mL bacteria.

the specimen and was calculated in milligrams of silver/grams of sample. Obviously, the cumulative amount of Ag^+ ions released from the samples occurred rapidly during the first 60 min after immersion in the releasing medium, and then increased gradually thereafter. The cumulative amount of Ag^+ ions released from the 30 min cross-linked fiber mat was greater than the amount released from samples cross-linked for 60 min and 120 min. This may be attributed to the fact that the degree of cross-linking is lower due to the short exposure time to glutraldehyde. This consequently leads to partial dissolution of polyvinyl alcohol from the nanofibers mats after a period of time then release more silver ions to the medium. The same proposed explanation is holds true for fiber mats cross-linked for 60 min but to a lesser extent. Specimens cross-linked for 120 min didn't dissolve and retained its morphological structure for three weeks. This suggests that in this case the fiber mats released silver ions by swelling mechanisms.

3.4. Antibacterial performance

The antibacterial activity of PVA/CS and PVA/CS/Ag-NPs fiber mats against *E. coli* was tested by using the viable cell-counting method. The effects of the composite fiber mats on the growth of the recombinant bacteria *E. coli* are shown in Fig. 9(a) and (b) shows the antibacterial activity of fiber mats obtained from various PVA/CS blends and exposed to different concentrations of bacteria. As shown in the plates, the number of bacteria colonies decreased by increasing the chitosan (CS) ratio in the fiber blend at concentrations of 7×10^5 CFU/mL (Fig. 9a). The same behavior was observed at bacterial concentration of 7×10^7 CFU/mL (Fig. 9b) but with lower efficiency. This suggests that fiber mats e-spun from PVA/CS blends of weight ratios of 90/10, 80/20, and 60/40 can stop to different extents the growth of *E. coli* for initial colony densities of at least up to 7×10^7 CFU/mL. Thus, the antibacterial activity of CS in the composite PVA/CS fibers is verified.

More importantly, the antibacterial activity of the PVA/CS/Ag-NPs fiber mats was measured and compared to that of PVA/CS systems. Fig. 9(c) and (d) illustrates the performance of fiber mats of PVA/CS-Ag-NPs with different PVA to CS weight ratios and different initial concentration of bacteria. Samples of *E. coli* with initial number concentration of 7×10^5 CFU/mL (Fig. 9c) and 7×10^7 CFU/mL (Fig. 9d) were completely eradicated when exposed to fiber mats with PVA/CS blend ratios of 80/20 and 60/40. However, there were some bacterial colonies still observed after application of fibers with reduced CS loading (blend ratio 90/10), for both bacterial concentrations. It is clear that at the same concentrations of bacteria, the antibacterial ability of the composite PVA/CS-Ag-NPs fiber mats increased with Ag-NPs loading. This suggests that the PVA/CS-Ag-NPs fiber mats with 20% or above CS concentration had bactericidal effects while fiber mats with lower CS content had bacteriostatic effects on *E. coli*. This demonstrates the superior antibacterial activity of the Ag-NPs in the composite PVA/CS-Ag-NPs fiber mats.

Two different mechanisms are proposed to be effective in the case of combination of chitosan and Ag-NPs. The antibacterial activity of chitosan is based on the damaging interaction of the polycation (protonated amino groups) with the negatively charged surfaces of bacteria, resulting in loss of membrane permeability, cell leakage, and finally cell death (Hang, 2010; Ignatova, 2006). On the other hand, Ag nanoparticles have stronger antibacterial properties because Ag nanoparticles attach to the cell walls and disturb cell wall permeability and cellular respiration (An, 2009; Son, 2006).

4. Conclusion

Silver nanoparticles, 20 nm average diameter, were successfully prepared in high concentration (3142 ppm) using green method. Chitosan was used as capping polymer and glucose was applied as reducing agent. Non-woven mats of PVA/CS blends and PVA/CS-Ag-NPs blends containing were successfully fabricated by the electrospinning method. PVA was partially miscible with CS and had good electrospinnability when blended with CS. The presence of Ag-NPs in the polymer blend solution of PVA and CS improved the electrospinnability of the blend. The formation of Ag-NPs on the surface of e-spun fibers was confirmed by obtaining TEM micrographs. The Ag-NPs in the PVA/CS-Ag-NPs blend solutions resulted in a reduction in the diameter of the e-spun fibers. The antibacterial experiment indicated that the e-spun mats of PVA/CS blends had good bactericidal activity against the Gram-negative bacteria *E. coli*. However, e-spun mats of PVA/CS-Ag-NPs blends were better. The presence of Ag-NPs in PVA/CS blend solutions enhanced not only the electrospinning performance but also the antibacterial ability of the e-spun mats which advocates a good wound dressing material.

Appendix A. Supplementary data

Supplementary data associated with this article can be found, in the online version, at http://dx.doi.org/10.1016/j.carbpol.2012.12.043.

References

Abdel-Halim, E. S.-D. (2011). Utilization of hydroxypropyl cellulose for green and efficient synthesis of Ag NPs. *Carbohydrate Polymers*, *86*, 1615–1622.

An, J. Z. (2009). Preparation and antibacterial activity of electrospun chitosan/poly(ethylene oxide) membranes containing silver nanoparticles. *Colloid and Polymer Science*, *287*, 1425–1434.

Anstas, P. a. (1998). *Green chemistry: Theory and practice*. New York: Oxford University Press, Inc.

Bŏzani'c, D. K.-B. (2011). Silver nanoparticles encapsulated in glycogen biopolymer: Morphology, optical and antimicrobial properties. *Carbohydrate Polymers*, *83*, 883–890.

Brett, D. W. (2006). A discussion of silver as an antimicrobial agent: Alleviating the confusion. *Ostomy Wound Management*, *52*, 34–41.

Choi, O. D. (2008). The inhibatory effects of silver nanoparticles, silver ions, and silver chloride colloids on microbial growth. *Water Research*, *42*, 3066–3074.

Dahl, J. A. (2007). Toward Greener Nanosynthesis. *Chemical Reviews*, *107*, 2228–2269.

Dongwei Weia, W. S. (2009). The synthesis of chitosan-based silver nanoparticles and their antibacterial activity. *Carbohydrate Research*, *344*(17), 2375–2382.

Goia, D. V. (2004). Preparation and formation mechanisms of uniform metallic particles in homogeneous solutions. *Journal of Material Chemistry*, *14*, 451–458.

Hang, A. T. (2010). E-spun mats of poly(vinyl alcohol)/chitosan blends containing silver nanoparticles: Fabrication and charachterization. *Carbohydrate Polymers*, *82*, 472–479.

Hebeish, A. A.-R.-M.-H. (2010). Carboxymethyl cellulose for green synthesis and stabilization of silver nanoparticles. *Carbohydrate Polymers*, *82*, 933–941.

Hebeish, A. E.-N.-D.-R. (2011). Highly effective antibacterial textiles containing green synthesized silver nanoparticles. *Carbohydrate Polymers*, *86*, 936–940.

Huang, H. a. (2004). Synthesis of chitosan-stabilized gold nanoparticles in the absence/presence of tripolyphosphate. *Biomacromolecules*, *5*(6), 2340–2346.

Hutchison, J. E. (2008). Greener nanoscience: A proactive approach to advancing applications and reducing implications of nanotechnology. *ACS Nano*, *2*(3), 395–402.

Ignatova, M. S. (2006). Electrospun nano-fiber mats with antibacterial properties from quaternised chitosan and poly(vinyl alcohol). *Carbohydrate Research*, *341*, 2098–2107.

Jia, Y. T. (2007). Fabrication and characterization of poly(vinyl alcohol)/chitosan blend nanofibers produced by electrospinning method. *Carbohydrate Polymers*, *157*, 454–459.

Kamyar, S. M. (2010). Green synthesis of silver/montmorillonite/chitosan bio-bionanocomposites using the UV irradiation method and evaluation of antibacterial activity. *International Journal of Nanomedicine*, *5*, 875–887.

Konwarh, R. K. (2011). Effect of sonication and aging on the templating attribute of starch for green silver nanoparticles and their interactions at bio-interface. *Carbohydrate Polymers*, *83*, 1245–1252.

Lim, S., & Hudson, S. M. (2004). Synthesis and antimicrobial activity of a water-soluble chitosan derivative with a fiber-reactive group. *Carbohydrate Research*, *399*(2), 313–319.

Park, W. H. (2004). Effect of chitosan on morphology and conformation of electrospun silk fibroin nanofibers. *Polymer*, *45*, 7151–7157.

Pastoriza-Santos, I. a.-M. (2002). Synthesis of silver nanoprisms in DMF. *Nano Letters*, *2*(8), 903–905.

Peresin, M. S. (2010). Nanofiber composites of polyvinyl alcohol and cellulose nanocrystals: Manufacture and characterization. *Biomacromolecules*, *11*(3), 674–681.

Pillai, C. K. (2009). Chitin and chitosan polymer: Chemistry, solubility and fiber formation. *Progress in Polymer Science*, *34*, 641–678.
Potara, M. J. (2011). Synergistic antibacterial activity of chitosan–silver nanocomposites on *Staphylococcus aureus*. *Nanotechnology*, *22*, 135101–135110.
Rabea, E. I. (2003). Chitosan as antimicrobial agent: Applications and mode of action. *Biomacromolecules*, *4*(6), 1457–1465.
Rujitanaroj, P. P. (2008). Wound-ressing materials with antibacterial activity from electrospun fiber mats containing silver nanoparticles. *Polymer*, *49*, 4723–4732.
Sakai, H. K. (2009). Preparation of highly dispersed core/shell-type titania nanocapsules containing a single Ag nanoparticle. *Journal of the American Chemical Society*, *128*, 4944–4945.
Sambhy, V. M. (2006). Silver bromide nanoparticle/polymer composites: Dual action tunable antimicrobial materials. *Journal of the American Chemical Society*, *128*, 9798–9808.
Sharma, V. Y. (2009). Silver nanoparticles: Green synthesis and their antimicrobial activities. *Advances in Colloid and interface Science*, *145*, 83–96.
Son, W. Y. (2006). Antimicrobial cellulose acetate nanofibers containing silver nanoparticles. *Carbohydrate Polymers*, *65*, 430–434.
Van Hyning, D. L. (2001). Silver nanoparticle formation: Predictions and verification of the aggregative growth model. *Langmuir*, *17*(11), 3128–3135.
Vigneshwaran, N. N. (2006). A novel one-pot green synthesis of stable silver nanoparticles using soluble starch. *Carbohydrate Research*, *341*,2012–2018.
Yanli, G. (2008). Preparation and characterization of heparinstabilized gold nanoparticles. *Journal of Carbohydrate Chemistry*, *59*(2), 171–178.
Zhou, Y. S. (2006). Electrospinning of chitosan/poly(vinylalcohol) acrylic acid aqueous solutions. *Journal of Applied Polymer Science*, *102*, 5692–5697.
Zhuanga, X. C. (2010). Electrospun chitosan/gelatin nanofibers containing silver nanoparticles. *Carbohydrate Polymers*, *82*(2), 524–527.